Adaptive Coherence Imaging System with Time-Domain Filtering

Yang Jiao, Sameer R. Bhalotra, Helen L. Kung, and David. A. B. Miller
Edward L. Ginzton Laboratory
Stanford University, Stanford, CA 94305-4085

The amount of coherence is an interesting property of a spectrum in its own right, regardless of the exact location of the coherent features [1-2]. In most spectral information extraction systems, the design starts by decomposing the scene into separate wavelength bins. The location of a peak in the spectrum is easily found, but much more effort is needed to determine the coherence level (narrowness of the spectral lines) of the source. We demonstrate an adaptive coherence imaging system that avoids decomposing the scene into separate wavelength bins. Rather, we decompose the scene into components distinguished by the level of their coherence, in the very early stages of the physical sensing process. Specifically, in an interferometric system, time domain filtering on a short piece of interferogram away from zero path length difference is performed during data collection. This enables the extraction of coherent spectral features in the spectrum, without ever determining the exact spectral location of the coherent features. The multispectral images of the scene are never fully constructed, yet we obtain an immediate indication of the presence of coherent features without a separate data-analysis system. Such an approach could be useful for distinguishing narrow spectral features, such as gasses, from the background, in a relatively simple spectrometer.

This architecture for discriminating narrow spectral features falls into the general framework of the time-domain filtering (TDF) architecture [3]. This makes the system more versatile than another methods of decomposing the scene into coherent and incoherent parts. We previously showed that a range of spectral feature discrimination tasks could be accomplished by recording a measurement waveform containing the spectral information from a source, and correlating the measurement waveform with appropriately chosen reference waveforms. The versatility lies in the fact that only the reference waveform needs to be changed in order for the TDF system to switch between different discrimination tasks. To switch the coherence imaging system into a system for discriminating between LED sources of different wavelengths is a trivial task [3]. The hardware for the TDF system remains the same - all that is needed is a different set of reference waveforms and interferometric scan parameters.

Time domain filtering on the interferogram is only one of the methods for decomposing the scene into coherent and incoherent parts. In an interval of an interferogram shifted far away from the zero displacement point, most of the energy will be from the high coherence spectral features. So another method would be squaring the interferogram and integrating over an interval away from zero displacement. In the same interval, simply looking for the presence of a AC signal as the spectrometer mirror is moved will also work. However, these methods are harder to implement in the TDF architecture, and may require normalization to prevent a high powered broadband source from been mistaken for a narrowband source. We choose the time domain filtering method to make the system more versatile.

The physical portion of the adaptive coherence imaging system is a interferometric imager. A lens system collects the light from the object. The light then passes through a 2-D raster scan galvano mirror set, which determines which pixel is sent through a Michelson interferometer. A piezo-electric transducer (PZT) actuator varies the path length of one interferometer arm. The interferogram for each pixel is converted to an electrical waveform by an amplified si photodetector. The PZT actuation, raster scanning, and data acquisition are controlled and synchronized by a PC.

The background of the scene of interest might be illuminated incoherently, but an effectively hidden element in the scene might have narrow spectral lines or be is illuminated by a narrowband source (e.g., an LED). For this method, we start by recording limited interferograms R_1 and R_2 for the narrowband source and a broadband background. The interferograms are recorded with only 4μm of optical path length difference, with the starting point shifted 15μm from the equal path length point. Using Gram-Schmidt orthogonalization [4], we find the vector space *S* that is spanned by R_1 and R_2. For each location (x,y) in the scene, we record a 4μm long interferogram $I_{x,y}$. We assume that the noise in the measurement waveforms are additive white Gaussian (AWGN), and that each spectral signature is equally likely to be the source of $I_{x,y}$. Then, we project $I_{x,y}$ into S for each location (x,y), compute the Euclidean distance between the projection and R_1, R_2, and pick the R_i closest to $I_{x,y}$ as the most probable spectra signature at location (x,y).

The 15μm displacement from zero optical path difference ensures that spectral features with a full-width-half-max (FWHM) of more than 30nm will have less than 0.1% of the energy left in the interferogram. In other words, the broadband background R_2 is mainly composed of measurement noise. If the noise is AWGN, most of its energy will not be in the bandwidth of the narrowband interferogram R_1, therefore, the measurement waveform $I_{x,y}$ for the broadband

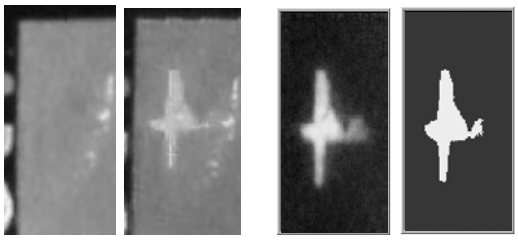

(a) (b) (c) (d)

Figure 1. (a) CCD image of scene illuminated with a tungsten lamp, and containing a weak image (an effectively hidden area) illuminated with an LED; (b) artificially enhanced CCD image showing hidden area with narrowband feature; (c) distance of $I_{x,y}$ to R_1(in the actual data); (d) Discrimination result from the actual data

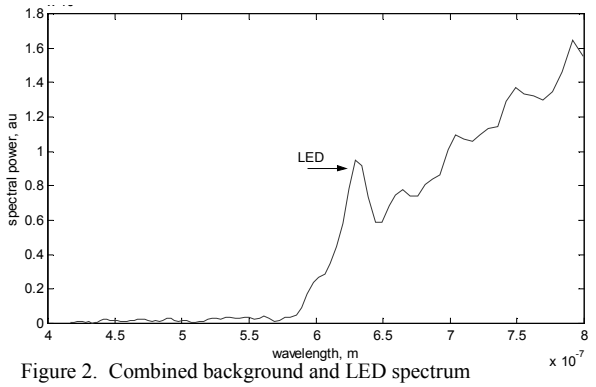

Figure 2. Combined background and LED spectrum

background would be mostly orthogonal to R_1. If R_1 is chosen, then the coherent spectral signature is most likely to be present. Because the interferogram is only 4μm long, the system responds to coherent features with in a 100nm interval around 600nm. The width and location of the interval can be changed by varying the length of the interferogram and the reference LED used. The sensitivity to a wide range of wavelengths characterizes the design philosophy of the system: we optimize the hardware to detect the presence of coherent features and skip the task of localizing the features in the spectrum.

The scene shown in Figure 1(a) has a red background printed on to a piece of white paper using a color printer, and illuminated by a tungsten lamp. The spectrum of the background is quite broad as shown in Figure 2. A cross-shaped aperture is taped to the back of the red paper, and a red LED illuminates the cross shaped area of the paper form the back. Figure 1(b) is a CCD image revealing the LED illuminated area by turning off the tungsten lamp and significantly increasing the power to the LED. Note that in Figure 1(a), the actual scene imaged by the coherence feature extraction system, the coherence part is not perceivable by neither the CCD camera nor the human eye.

Figure 1 c), d) show the result of the coherence feature extraction. Note that the Euclidean distance to the coherence reference waveform already visually reveals the coherent cross object. The lighter areas in Figure 1c) indicate that the measurement waveform is close to the coherent reference waveform, i.e. these areas contain coherent spectrum features. The distance values in Figure 1c) are analog and are prone to subjective interpretation. Comparing the distances to R_1 and R_2, Figure 1d) shows the binary decision of which area has a high likelihood of containing the coherent signature. It closely matches the artificially enhanced image of the cross in Figure 1b).

The speed which this data is acquired illustrates the advantage of the coherent imaging architecture. Because the coherent imaging setup only needs an interferogram with 4μm of optical path length difference, the acquisition of the image took about 1 minute (taken one pixel at a time). The 15μm displacement from zero path difference extracts spectral features with a width less than 30nm. If the interferometric system is to find the coherent spectral feature by profiling the spectrum, it needs to have a spectral resolution of at least 30nm, which would require a scanning length of roughly 16μm. Using the same experimental setup with the PZT mirror actuator, acquiring that data would take 4 times as long.

In summary, for some sensing applications, even the seemingly fundamental process of breaking a spectrum into frequency components may not be the best way to look for features in the spectrum. We have demonstrated the coherent imaging architecture, with inherent decomposition of the image into coherent and incoherent components. The decomposition at a very early stage of the physical measurement process means that 1) minimal data analysis is needed, and 2) the system never needs to have the resolution that would conventionally be required to resolve the spectral features of interest. These advantages translate into relaxed requirements on the hardware design and faster data collection, and will aid the design and expand the applications of inexpensive, mobile hyperspectral and multispectral imaging systems.

This material is based upon work supported by the Unites States Air Force under contract No. F49620-00-C-0040. Support was provided by a DARPA grant for Photonic Wavelength And Spatial Signal Processing, under a sub contract from FMA&H. YJ acknowledges the support of the NSFGRF and the Reed-Hodgson Stanford Graduate Fellowship. SRB gratefully acknowledges the support of the Regina Casper Stanford Graduate Fellowship.

[1] B. Moeremans, “The use of ERS SAR interferometric coherence to evaluate crop height,” Proc. of the First International Conference on Geospatial Information in Agriculture and Forestry, 485-492 (1998).

[2] D. Huang, E. A. Swanson, C. P. Lin, J. S. Shuman, W. G. Stinson, W. Chang, M. R. Hee, T. Flotte, K. Gregory, C. A. Pulia¯to, and J. G. Fujimoto, “Optical Coherence Tomography," Science, vol. 254, pp. 1178-1181, Nov. 1991.

[3] S. R. Bhalotra, H. L. Kung, Y. Jiao, and D. A. B. Miller, "Adaptive time-domain filtering for real-time spectral discrimination in a Michelson interferometer," Opt. Lett., 27, 1147-1149 (2002).

[4] J. Proakis and M. Salehi, Communication Systems Engineering. Prentice Hall, New York, 1994